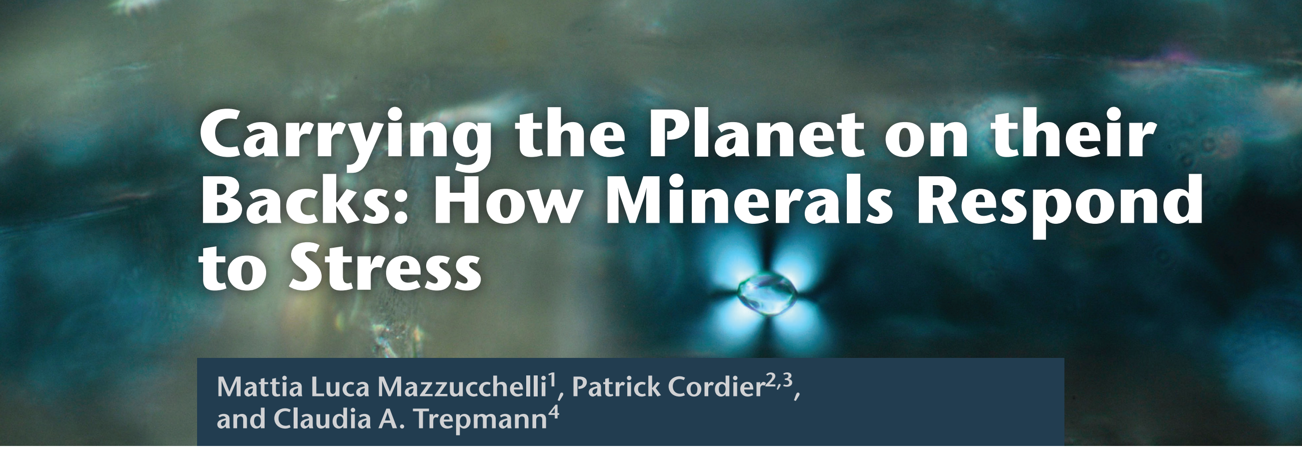

Carrying the Planet on their Backs: How Minerals Respond to Stress

Mattia Luca Mazzucchelli[1], Patrick Cordier[2,3], and Claudia A. Trepmann[4]

Coesite inclusion in garnet viewed under crossed polarizers, showing birefringent halos in the host garnet induced by residual stress. PHOTO: N. CAMPOMENOSI.

1811-5209/26/0022-096$2.50 DOI: 10.2138/gselements.22.2.96

Far from being passive building blocks, minerals govern how Earth evolves and deforms, from seismic wave propagation to rock deformation and plate motion. This article explores how pressure builds within Earth and how minerals' elastic response to compression and seismic waves reveals its internal structure. At higher stresses, beyond their elastic limit, deformation in minerals becomes permanent through crystal plasticity created by crystal defects and strongly enhanced by temperature. Over geological time scales, aggregates of crystals behave effectively as highly viscous fluids, enabling mantle convection and plate dynamics. Understanding Earth's large-scale behavior therefore requires linking rock rheology to the mechanics of minerals down to crystal defects. By integrating observations, experiments, and models, we uncover the hidden rules connecting atomic interactions to planetary dynamics.

Keywords: elasticity; rheology; stress; strain

MINERALS AND ROCKS UNDER GRAVITY

To a first approximation, the Earth is a gravitating, self-compressed body (Turcotte and Schubert 2002). Gravity draws particles inward, while interatomic forces, described by interatomic potentials (FIG. 1), oppose further compression. This interplay creates pressure that ensures that every point of the Earth remains in mechanical equilibrium by counterbalancing the inward gravitational forces with an outward pressure gradient. As a result, pressure and density must increase with depth in the Earth, and this is confirmed by comparing the mean density of the Earth (~ 5,500 kg/m^3), obtained by the ratio of the mean mass of the Earth to its volume, and the average density of rocks at the Earth's surface (~ 2,700 kg/m^3). Most of the Earth's interior consists of minerals, and understanding their response to temperature (T), pressure (P), and non-hydrostatic stress (see BOX 1 for the definition of hydrostatic P and stress) is crucial to inferring the planet's internal structure. One key property is compressibility, which measures how a material's volume and density change under P. More than 100 years ago, Williamson and Adams (1923) had already realized that the compressibility of a homogeneous mantle could not explain the Earth's density profile, suggesting instead an internal structure with denser phases at greater depths.

The elastic response of minerals gives us a way to image the structure of the inaccessible inner part of the Earth. Earthquakes generate seismic (i.e., mechanical) waves, which impose stresses on minerals lasting seconds to minutes. Under low differential stress (see BOX 1) and short time scales, minerals behave elastically: atoms are displaced only slightly from their equilibrium positions, and the interatomic forces restore them to their initial positions once stress is removed (FIG. 1). By experimentally determining the elastic properties of the minerals that compose the Earth, we can derive seismic wave velocities of rocks, and, in turn, when the velocity, amplitude, and frequency of seismic waves are measured through seismometers, we can infer the structure, density, and mineralogy of the inner parts of the Earth (FIG. 2).

Single Crystal Elasticity

The linear elastic behavior of an ideal, isotropic solid at a given P and T is described by just two **elastic moduli***. The bulk modulus controls how much its volume changes under hydrostatic P. The shear modulus governs how the solid responds to a shear (shape-changing) stress. However, minerals are elastically anisotropic: their response to stress depends on direction within the crystal. Depending on their crystal symmetry, up to 21 independent elastic moduli are required to capture their full anisotropic elastic and seismic response at a given P and T (Cordier and Jackson 2026 this issue). Temperature also affects elastic behavior by causing thermal agitation, which displaces atoms from equilibrium. Interatomic forces act to restore equilibrium, resulting in atomic oscillations. Ideally, this leads to harmonic motion (FIG. 1A, blue dashed line) with no volume change. However, real crystals show anharmonicity (FIG. 1A, blue solid line; Anderson 1995), which leads to thermal expansion and affects both the elastic and thermal properties of minerals (Jackson et al. 2026 this issue).

A major challenge in determining the elastic properties of minerals in planetary studies is to reproduce the high P and T of Earth's (or other planets) interior. With devices such as multi-anvil presses and diamond anvil cells, P can be gradually increased to tens or even hundreds of gigapascals while concomitant heating can raise T to thousands

1 Université de Lausanne - Institute of Earth Sciences
CH-1015 Lausanne, Switzerland
E-mail: mattia.mazzucchelli@unil.ch

2 Université de Lille - Unité Matériaux et Transformations UMR CNRS 8207
59655 Villeneuve d'Ascq Cedex, France
E-mail: patrick.cordier@univ-lille.fr

3 Institut Universitaire de France
75005 Paris, France

4 Ludwig-Maximilians-Universität München
Department für Geo- und Umweltwissenschaften
DE-80333 München, Germany
E-mail: claudia.trepmann@lmu.de

* Definitions of terms presented in **blue** are given in the glossary on page 81.

Box 1 WHAT IS STRESS?

Stress is an abstract concept used to describe how forces act in matter, which is considered to be a continuous medium. At a point M inside the solid and on a facet oriented by the vector $\vec{n}$, there is a surface density of forces $\vec{T}$ (traction vector) acting on this elementary surface, which is defined by:

$$\vec{T} = \bar{\bar{\sigma}}(M) \cdot \vec{n}$$

where $\bar{\bar{\sigma}}$ is a second-rank tensor called the Cauchy stress tensor. This tensor expresses completely the local stress state at M. To fully describe this state using the three axes of a Cartesian coordinate system (123), six stress components are required: three normal components denoted σ_{11}, σ_{22}, and σ_{33} and three shear components σ_{12}, σ_{13}, and σ_{23}. The stress tensor can therefore be represented by a matrix with three rows and three columns that is symmetrical ($\sigma_{ij} = \sigma_{ji}$) to respect equilibrium.

$$\bar{\bar{\sigma}}(M) = \begin{pmatrix} \sigma_{11} & \sigma_{12} & \sigma_{13} \\ \sigma_{21} & \sigma_{22} & \sigma_{23} \\ \sigma_{31} & \sigma_{32} & \sigma_{33} \end{pmatrix}$$

It is always possible to decompose a given stress tensor into an isotropic (also called hydrostatic, or spherical) part and a deviatoric part:

$$\begin{pmatrix} \sigma_{11} & \sigma_{12} & \sigma_{13} \\ \sigma_{21} & \sigma_{22} & \sigma_{23} \\ \sigma_{31} & \sigma_{32} & \sigma_{33} \end{pmatrix} = \begin{pmatrix} \sigma_h & 0 & 0 \\ 0 & \sigma_h & 0 \\ 0 & 0 & \sigma_h \end{pmatrix} + \begin{pmatrix} \sigma_{11} - \sigma_h & \sigma_{12} & \sigma_{13} \\ \sigma_{21} & \sigma_{22} - \sigma_h & \sigma_{23} \\ \sigma_{31} & \sigma_{32} & \sigma_{33} - \sigma_h \end{pmatrix}$$

with $\sigma_h = \frac{1}{3}(\sigma_{11} + \sigma_{22} + \sigma_{33})$. The sum of all diagonal terms of the stress tensor is independent of the coordinate system, implying that σ_h does not depend on the orientation. However, the individual components of the stress tensor depend on the coordinate system. There exists a specific reference frame in which the shear stress components vanish. In this orientation, the stress tensor is diagonal, with σ_1, σ_2, and σ_3 designated as principal stresses and the corresponding reference axes (1′2′3′) are termed principal axes.

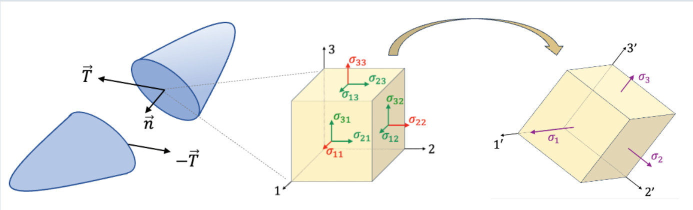

The hydrostatic part contains no shear components, and in isotropic materials is responsible for volume changes only. The deviatoric part is responsible for the change of shape, and its trace is always equal to zero. Differential stress, defined as the difference between the maximum and minimum principal stresses ($\sigma_{max} - \sigma_{min}$), is commonly used to quantify deviations of the stress state from a hydrostatic condition. It is important to distinguish between a general stress state (comprising both a hydrostatic and deviatoric part), and a purely hydrostatic state (i.e., P) that is described by an isotropic stress tensor:

$$\begin{pmatrix} -P & 0 & 0 \\ 0 & -P & 0 \\ 0 & 0 & -P \end{pmatrix}$$

Both the stress components and pressure are described using the same units (the pascal, Pa). Here we use the positive sign convention implying that a positive normal stress, σ, points away from the stress element. Tension is positive, while compression is negative. Using this convention, pressure P, conventionally taken as a positive quantity upon compression, is given a minus sign (i.e., $P = -\sigma_h$). The convention that structural geologists use, whereby $\sigma_1 > \sigma_2 > \sigma_3$, derives from Anderson's theory (in which compressional stresses are assumed as positive). This explains the three tectonic regimes in the upper crust: extension $\sigma_1 = \sigma_v$ (normal faults), contraction $\sigma_3 = \sigma_v$ (thrust faults), and strike-slip $\sigma_2 = \sigma_v$ (strike-slip faults), where σ_v is the vertical stress.

of kelvin. Bulk elastic properties and variations of volume are measured with techniques such as X-ray diffraction. Anisotropic elastic properties are typically obtained by measuring the velocity of acoustic waves propagating through the material, or the scattering of an incident light beam that interacts with the normal modes of vibration of the crystal (Bass and Zhang 2015). Laboratory measurements of the elastic properties of minerals are essential

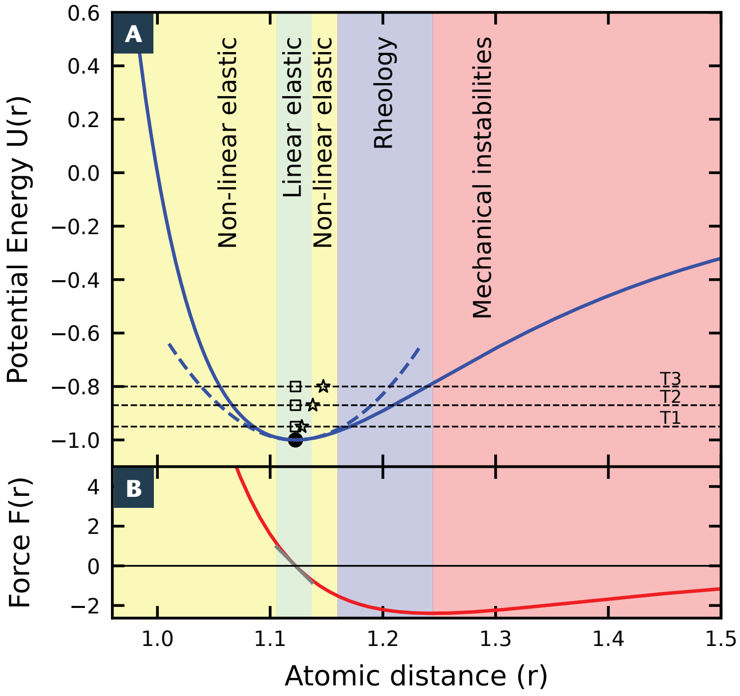

FIGURE 1 (**A**) Energy from the Lennard–Jones interatomic potential (blue line) and (**B**) corresponding force (red line) as functions of interatomic radial distance *r*. The plot is presented in reduced Lennard–Jones units (Frenkel et al. 1996) where the energy parameter and length scale of the potential are set to unity, preserving the physical meaning of the potential in non-dimensional units. Although the model describes the interaction of just two atoms, it provides qualitative insight into the response of minerals to variations in *P*, *T*, and deformation. For small displacements from equilibrium (black dot in **A**), the potential is nearly harmonic (blue dashed line in **A**), giving a linear force–displacement relation (grey line in B) that defines linear elasticity in minerals (green region). At larger displacements (yellow region), the response is still reversible (elastic) but becomes nonlinear, as observed in high-*P* mineral experiments. At very large displacements (violet, red regions), permanent changes are developed such as bond breaking, dislocation motion, or diffusion. Increasing temperature from T1 to T3 increases vibrational amplitude. In an idealized harmonic model (blue dashed line in **A**), the mean interatomic distance remains constant with temperature (black squares in **A**), implying no thermal expansion. In real materials, the anharmonicity makes vibrational frequencies depend on volume, driving thermal expansion. In a biatomic interaction, where the anharmonicity of the potential is reflected in its asymmetry, the increase in mean interatomic distance with temperature is shown by black stars in **A**.

for constructing physically based models that describe the elasticity of minerals in the Earth's interior and allow for extrapolation to extreme conditions at which accurate measurements are difficult to obtain. Equations of state, which account for the non-linear elastic response at large **strains** (FIG. 1B), relate volume, compressibility, and thermal expansion to P and T while enforcing specific thermodynamic relationships (Birch 1952; Anderson 1995; Angel et al. 2014). Elastic properties also vary with chemical composition and crystal structure. Laboratory measurements and first-principles calculations (Prencipe 2019) provide elastic properties and P-derivatives for mineral end-members as well as for solid solutions, with T-derivatives constrained experimentally. These results are included in self-consistent databases, from which phase diagrams for typical compositions of the Earth's interior, together with their elastic and seismic properties, can be calculated (e.g., Connolly 2005).

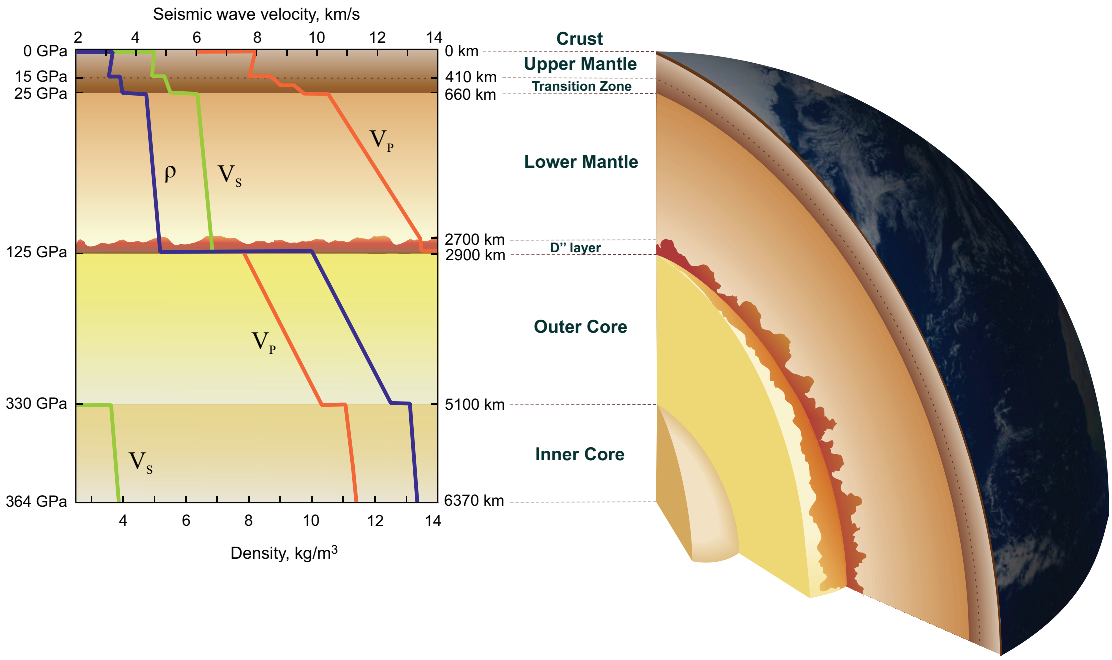

FIGURE 2 Radial profiles of the Preliminary Reference Earth Model (PREM; Dziewonski and Anderson 1981), showing P-wave velocity (Vp), S-wave velocity (Vs), and density (ρ) as functions of Earth's radius. Discontinuities in such properties provide fundamental first-order information on the inner structure of the Earth. COURTESY OF A.M. GORYAEVA.

From Crystals to Rocks: Effective Properties of Aggregates

Seismic waves travel through Earth with wavelengths on the order of kilometers, therefore sampling the combined elastic response of many mineral grains bound together in rocks. The effective elastic and seismic responses of an aggregate differ from those of individual grains, and depend on the properties, volume fractions, and exact arrangement of its constituent grains. An aggregate of randomly oriented anisotropic grains behaves approximately isotropically, allowing for the use of simple models (e.g., Voigt and Reuss bounds) to estimate the effective elastic properties. However, the shape and/or crystallographic preferred orientations of minerals and other anisotropies (e.g., systematic sets of fractures, material layering, etc.) can strongly affect the elastic response, and more sophisticated models are necessary to describe the resulting effective anisotropic elasticity (Mavko et al. 2020). Once the effective bulk and shear moduli of a polymineralic rock are determined, the propagation velocities of compressional and shear waves can be calculated. However, as seismic waves propagate, part of their energy is attenuated via anelastic damping (Jackson 2015), meaning that the response is not purely elastic. This attenuation arises because, at low frequencies, under relatively high stress, and at elevated T, features such as point defects, dislocations, grain boundaries, and small fluid fraction present at grain contacts (melts or metamorphic fluids) also respond with some delay to stress variations. Therefore, even at relatively short time scales, the **macroscopic** response of mineral aggregates becomes visco-elastic and time dependent.

The Inner Structure of the Earth Revealed from Seismic Waves

Integrating our knowledge of the physical response of minerals under P and non-hydrostatic stress with seismic observations has been fundamental in revealing the Earth's inner structure. Birch (1952) pioneered the approach of comparing seismic velocities with the elastic properties of candidate materials to infer the composition of Earth's interior. For example, seismic discontinuities, defined by sharp variations in wave velocities with depth (FIG. 2), are often interpreted to correspond to mineral phase transitions by comparison with high P–T experimental results, thus providing direct constraints on the mantle's T and mineralogy at specific depths (e.g., Stixrude 2015). The inversion of seismic observations (travel times, free oscillation frequencies, and waveform data) and astronomical data (Earth's radius, mass, and moment of inertia) together with the physical properties of minerals allows construction of seismological models that are the basis for seismic tomography and geophysical studies. For decades, the Preliminary Reference Earth Model (PREM) of Dziewonski and Anderson (1981) has been the standard one-dimensional seismic model. This spherically symmetric model characterizes the average elastic properties, seismic velocities, density, and attenuation as functions of radius (FIG. 2). With advances in both laboratory measurements and seismic observational techniques, modern studies now constrain not only radial but also lateral variations in seismic wave velocities, leading to the development of comprehensive three-dimensional models of the Earth's structure (Stixrude 2015).

EVERYTHING FLOWS: FROM THE PLANETARY SCALE TO GRAINS AND DEFECTS AND BACK

Seismology gives a "snapshot" of Earth's internal structure, but our planet is far from static. At depth in the Earth's upper crust, brittle deformation nucleates upon stress loading above the elastic limit of geomaterials, triggering earthquakes. In the lithosphere, deformation is localized especially at, but not restricted to, tectonic plate margins such as rift zones and subduction zones. Observations from rocks exhumed from larger depths in mountain belts and shear zones show that deeper in the lithosphere, at higher T, rocks flow in the solid state. The dynamics of the Earth is largely governed by the **viscosity** of the mantle (Turcotte and Schubert 2002), which controls **convection** and the transfer of material and heat between the core and surface (Jackson et al. 2026 this issue).

Therefore, to understand the Earth's large-scale dynamics, we need to link the behavior of large rock volumes to processes on the mineral scale and down to the scale of defects in crystals. Remarkably, an aggregate of solid crystals can behave like a highly viscous fluid when averaged over kilometers and millions of years, whereas the fundamental mechanisms and processes occur in individual crystals on time scales of seconds. A striking example is the bridgmanite–post-perovskite (ppv) transition in the D″ region just above the core–mantle boundary

(Fig. 2). Ppv crystals develop strong crystallographic preferred orientations (CPO) due to their layered structure, accommodating large deformations by dislocation slip (Wu et al. 2017). The collective behavior of ppv crystals thus reduces viscosity and generates seismic anisotropy, affecting mantle convection and core–mantle interaction. **Flow laws** are empirical equations obtained from experiments that capture this collective behavior of **microscopic** processes (Turcotte and Schubert 2002). They relate stress to **strain rate** by incorporating the contributions of specific microscopic mechanisms into a set of parameters, therefore describing the effective viscosity of rocks. As such, they are an essential ingredient of any quantitative continuum-mechanical description of the deformation and dynamics of the Earth. Yet, this macroscopic rheological behavior relies on the fundamental mechanisms and processes operating in single crystals and aggregates, and the two scales are coupled through direct feedback.

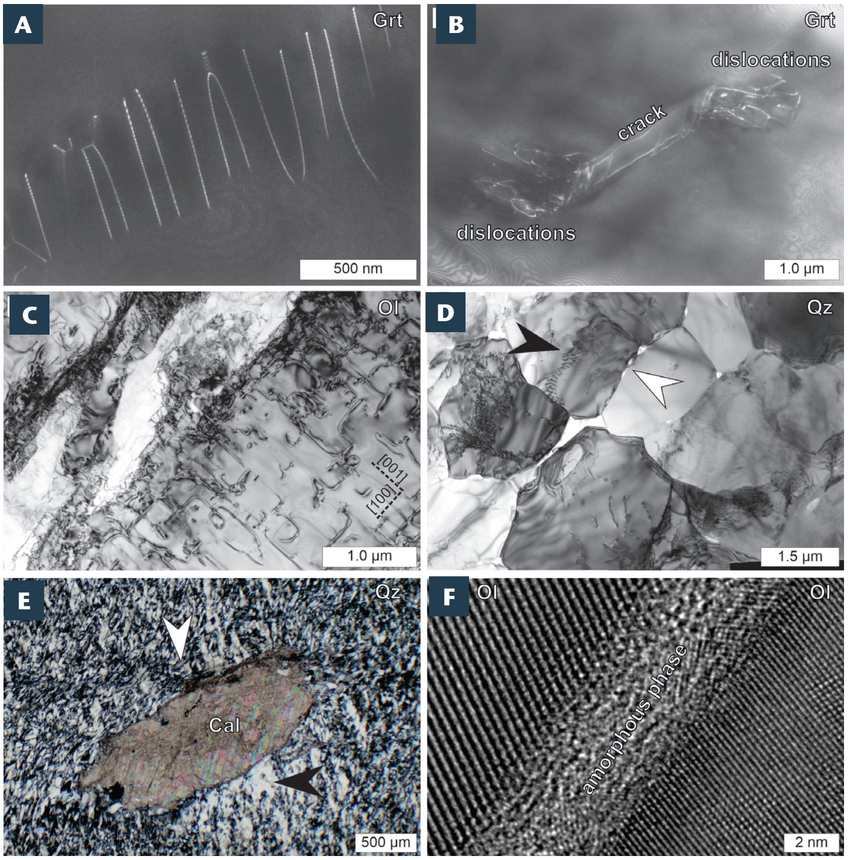

Figure 3 Dislocations and boundaries in deformed minerals and rocks. (**A**) Low-angle grain boundary in garnet, eclogite from Braganza, Portugal. Peak conditions estimated at 1000 °C, 2 GPa confining pressure (TEM weak-beam dark-field image). Image courtesy of V. Voegelé. (**B**) Crack in garnet deformed experimentally at 900 °C and 6.5 GPa confining pressure in a multianvil apparatus. Dislocations are emitted due to stress concentration at the crack tips (TEM weak-beam dark-field image). Image courtesy of V. Voegelé. (**C**) Heterogeneous dislocation density in experimentally deformed olivine at 600 °C, 1 GPa confining pressure and maximum differential stresses of 1.3 GPa, followed by annealing at 800 °C for 16 h (TEM bright-field image). (**D**) Grain microstructure of naturally deformed quartz in a mylonite (TEM bright field image, sample CT277, Sesia Zone, Western Alps) with low-angle grain boundary (black arrow) and high-angle grain boundaries partly decorated by fluid inclusions (white arrow). (**E**) Polarized light micrograph (crossed polarizers) of recrystallized quartz aggregate shown in (**D**), with grain size, shape and orientation influenced by inclusion of twinned calcite (Cal), indicating local stress/strain concentration (white arrow) and stress/strain shadow (black arrow). (**F**) Amorphized grain boundary in an olivine aggregate deformed in a Paterson press at 950 °C, 300 MPa confining pressure, differential stress 1.6 GPa (HRTEM). Image courtesy of V. Samae.

How Do Minerals React to Stresses Higher than Their Elastic Limit?

The elastic, reversible response of minerals is restricted to low differential stress (Fig. 1). Beyond the elastic limit, deformation becomes permanent and is accommodated by mechanisms of crystal **plasticity**, which are strongly *T*-dependent. In this regime, minerals can accumulate crystal defects (Fig. 3A–3C), which are deviations from their ideal crystallographic structure. For example, a point defect refers to a missing (vacancy) or misplaced (interstitial) atom in the otherwise regular crystallographic structure. Dislocations are linear defects that, by moving in certain planes (known as slip planes), shear the crystal by an elementary amount called the Burgers vector ($\vec{b}$). As such, they are the agents of crystal plastic deformation and can be seen using transmission electron microscopy (TEM, Fig. 3A–3D). They are generated upon stress concentrations at discontinuities, for example, at the tip of microcracks (Fig. 3B). Upon their movement through the crystal, they interact with each other, commonly leading to a heterogeneous spatial distribution and to heterogeneously strained crystals (Fig. 3C, 3D). Dislocations can arrange into low-angle grain boundaries to reduce the elastic energy associated with these defects (Fig. 3A, 3D). Moreover, rocks are composed of aggregates of grains and various mineral phases and their boundaries become important locations to accommodate strain (Fig. 3D–3F). Strain-induced grain boundary migration, i.e., dynamic recrystallization, modifies the grain boundary network during deformation, continuously renewing the microstructure and controlling grain size evolution. Boundaries of any type are essential in the macroscopic deformation behavior of rocks, during dislocation **creep** (with dynamic recrystallization; Fig. 3D, 3E), high-stress crystal plasticity (with formation of twin boundaries and cracks; Fig. 3B), as well as dissolution–precipitation creep (Gratier et al. 2013). In addition, grain boundaries accommodate strain through grain boundary sliding, and can host disclinations that play a key role in localizing deformation at the nanoscale (Cordier et al. 2014). Grain boundaries can be both sites of stress/strain concentrations (Fig. 3E, white arrow) as well as sites of stress/strain shadows (Fig. 3E, black arrow), depending on the differences in flow strength of adjacent minerals and on the orientation of the boundaries to the local stress/strain field. Observation of boundaries at all scales, from **polarized light microscopy** (Fig. 3E) to TEM (Fig. 3D), gives us relevant information on their role in the rheology of rocks. Yet, the real structure of boundaries is resolvable only by high-resolution TEM (Fig. 3F).

What are the Stresses in the Earth's Interior?

The presence of Earth's topography together with the associated crustal-thickness variations suggest that, on average, the lithosphere experiences and sustains differential stresses (Moulas et al. 2019). Minerals may develop and sustain significant levels of non-hydrostatic stress, as evidenced from observations on deformed rocks (Fig. 4). For example, electron tomography of [001] dislocations in olivine and field dislocation mechanics have revealed significant variations in the local resolved shear stresses (RSS) on various slip planes on the order ± 400 MPa (Weidner et al. 2024). Such observations allow us to directly investigate the build-up of kinematic hardening and the activation of different dislocation slip systems during deformation. Moving up in scale from individual crystals to mineral aggregates, we observe that rocks may develop non-hydrostatic stresses upon variations of external *P* and *T* due to the heterogeneous physical properties of the constituent minerals. For example, due to contrasts in thermo-mechanical properties, minerals included in other host minerals can develop over- or under-pressures exceeding 1 GPa during burial and exhumation (Angel et al. 2015). Residual pressures measured in inclusions (e.g., by **Raman spectroscopy**, Solomatova et al. 2026 this issue), can be used in inversion models to constrain the pressure of metamorphism and differential stress during geological processes (e.g., Zhong et al. 2021). Metamorphic reactions associated with volume changes, such as the phase transition from coesite to quartz in a polyphase rock during exhumation from ultrahigh-pressure metamorphic conditions, can impose local and short-term differential stresses of several hundred MPa on the surrounding crystals (e.g., Lenze et al. 2005, Fig. 4). On a larger scale, transient differential stresses on the order of hundreds of MPa to GPa and fast strain rates (on the order of 10^{-5} s^{-1}) occur especially during the seismic cycle even below the Earth's upper seismogenic zone from depths at greenschist facies conditions to mantle depths (Fig. 4 (4–7)), as indicated for example by minerals containing twins with high critical resolved shear stress (CRSS) and/or pseudotachylytes. Also, at slower strain rates (on the order of 10^{-12} s^{-1} to 10^{-14} s^{-1}), rocks can experience differential stresses of a few tens to hundreds of MPa, as indicated from deformed rocks exhumed from large depths in combination with experimental rock deformation (Fig. 4).

BEHAVIOR UNDER HIGH STRESS

Minerals are observed to sustain high differential stresses, raising the question of the maximum strength of a defect-free crystal, or one in which defects are inactive, for instance due to the stress time being too short in relation to the response time. Hypervelocity impacts of large asteroids on the Earth's surface trigger shock waves with dynamic stress conditions that last for fractions of a second to a few seconds. Traveling faster than the local speed of sound, a shock wave creates a sharp discontinuity in *P*, *T*, and density, usually involving irreversible transformations, which makes it different from elastic waves. These shock waves also generate extremely high deviatoric stresses, as indicated by minerals containing twins with high CRSS values (Fig. 4). These intense, short-lived stresses can drive phase transformations, up to melting or vaporization, with the brief duration of the pressure pulse playing a critical role in the transformation process. Early studies found high-pressure silica polymorphs (coesite, stishovite) in impact craters like Meteor Crater (Arizona, USA). The transformation pathways during these very intense but very brief events can be unusual. For example, advanced time-resolved experiments in modern synchrotron facilities have revealed an ultrafast transformation pathway in silica that includes a new intermediate rosiaite-type phase (Otzen et al. 2023). Moreover, minerals may undergo martensitic transformations by diffusionless mechanisms, where deformation and polymorphic phase transitions occur simultaneously, as exemplified by the shock-induced transformation of rutile (Langenhorst and Deutsch 2012). As bonds are stretched, the interatomic force increases to a maximum and then decreases (Fig. 1), marking the onset of bond instability. In a crystalline structure, this can lead to more complex and unexpected behaviors. Under extreme shear, atoms can form new bonds, leading to exceptional strain hardening. This is the case of enstatite (Gouriet et al. 2022), which forms a new, extremely resistant phase when subjected to uniaxial tension (Fig. 5). These considerations raise the question of how the description of thermodynamic equilibria and phase diagrams should incorporate the effects of non-hydrostatic stress states in addition to hydrostatic pressure.

Beyond the instability threshold, predicting outcomes is difficult: very short durations and low *T* hinder transformation kinetics and may prevent the formation of stable phases. A frequently observed response of minerals is the disruption of long-range crystalline order (i.e., amorphization). The resulting amorphous material may have struc-

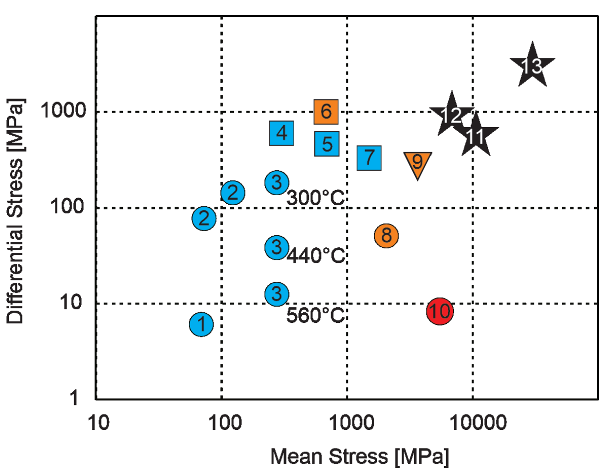

Figure 4 Stresses prevailing in the Earth: tectonic flow stresses (circles), transient coseismic stresses (squares), transient stresses upon local phase transformations (triangle) and stresses from hypervelocity impacts (stars). Blue colors correspond to upper to middle crustal levels, orange colors to lower crustal levels and subduction zones, and red colors to asthenosphere. (1) Salt dome tectonics, halite subgrain size. (2) KTB borehole. (3) Tonale mylonites, 300 °C, 440 °C, and 560 °C, quartz recrystallized grain size. (4) Thrust fault, pseudotachylytes 300–400 °C, amphibole twins. (5) Strike-slip, mylonites, 300–400 °C, jadeite twins. (6) Lower continental crust, pseudotachylytes, 650–750 °C, pyroxene twins. (7) Subduction zone, pseudotachylytes, 470 °C, volume of pseudotachylyte. (8) Subduction channel, UHP granite 600 °C, quartz foam structure. (9) Subduction channel, UHP, 700–800 °C, jadeite twins, coesite-quartz transformation. (10) Asthenosphere, low strain rates (ca. 10^{-15} s^{-1}), viscosities of 10^{21}–10^{22} Pas. (11) Ries impact breccia: maskelinite, amphibole twins. (12) Mechanical (0001) Brazil twins in shocked quartz from the Rochechouart impact structure, France. (13) Numerical impact model of the stress-strain during shock metamorphism. Data sources are provided in the online supplement.

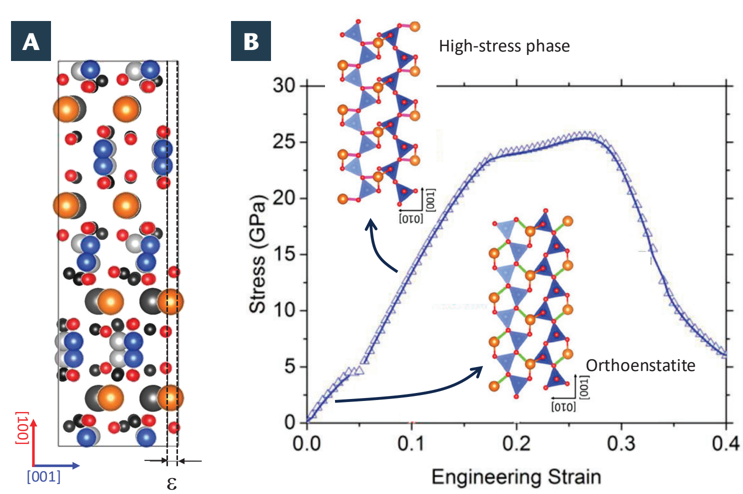

Figure 5 Theoretical behavior of enstatite under uniaxial tension. Ab initio calculation procedure. (**A**) A unit cell of enstatite is stretched along the [001] direction. (**B**) The uniaxial stress–strain curve obtained from ab initio calculations shows a change in slope during the formation of the new phase, which leads to the formation of new bonds (shown in red). This phase only becomes mechanically unstable at very high stresses of 25 GPa. Modified after Gouriet et al. (2022).

tural and rheological characteristics quite different from quenched melts, as is observed in diaplectic glasses from impact craters. They also behave very differently from crystals, generally accommodating greater deformation. A clear example is the amorphization of grain boundaries in olivine under high stresses (Fig. 3F), which promotes grain boundary sliding (Samae et al. 2021).

PERSPECTIVES: THE INTERPLAY BETWEEN STRESS, MINERAL EQUILIBRIA, AND REACTIONS

The coupled feedback between the mechanical state of rocks, phase transitions, and chemical reactions control many geological processes investigated across multiple disciplines. They include the reactive transport in the lithosphere, equilibria and microstructures in rocks, and rock rheology, among others, with implications for lithospheric evolution, reservoir stability, and earthquake cycles (e.g., Gratier et al. 2013). Thermodynamic equilibria in the Earth are commonly interpreted assuming that stresses are hydrostatic and locally homogeneous (e.g., Connolly 2005). However, stresses in rocks are often heterogeneous and non-hydrostatic (Fig. 4), and the extent to which they influence mineral equilibria and reactions remains an active area of research. At the atomistic scale, both the mechanical state and thermodynamic equilibria are governed by the same underlying physical forces (e.g., Frolov and Mishin 2010). Yet, in practice, the appropriate thermodynamic framework for deforming systems remains debated (e.g., Hobbs and Ord 2016; Powell et al. 2018; Wheeler 2020; Mazzucchelli et al. 2026), and the magnitude of non-hydrostatic stress effects on phase stability and reactions has yet to be fully quantified. Experimental studies of phase transitions and dissolution–precipitation creep under differential stress have provided important insights, yet the underlying theoretical frameworks remain incomplete. Developing predictive descriptions of stress–reaction coupling in Earth materials will likely require closer integration of thermodynamics, solid-state physics, and materials science.

ACKNOWLEDGMENTS

P. Cordier has received funding from the European Research Council (ERC) under the European Union's Horizon 2020 research and innovation programme under grant agreement No 787198 – TimeMan. We thank S. Demouchy and F. Langenhorst for their constructive reviews, which improved the clarity of this article. We also acknowledge R. J. Angel and J. P. Gonzalez for their comments on an earlier version of the manuscript, and N. Campomenosi for providing the banner image. The editorial handling of S. Chakraborty and J. M. Jackson is greatly appreciated.

For supplemental material, visit elementsmagazine.org/supplements/.

REFERENCES

Anderson OL (1995) Equations of State of Solids for Geophysics and Ceramic Science. Oxford University Press, 405 pp

Angel RJ, Alvaro M, Gonzalez-Platas J (2014) EosFit7c and a Fortran module (library) for equation of state calculations. Zeitschrift für Kristallographie - Crystalline Materials 229: 405-419, doi: 10.1515/zkri-2013-1711

Angel RJ, Nimis P, Mazzucchelli ML, Alvaro M, Nestola F (2015) How large are departures from lithostatic pressure? Constraints from host–inclusion elasticity. Journal of Metamorphic Geology 33: 801-813, doi: 10.1111/jmg.12138

Bass JD, Zhang JS (2015) Theory and practice: techniques for measuring high–P–T elasticity. In Schubert G (ed) Treatise on Geophysics (Second Edition). Elsevier, Oxford, pp 293-312, doi: 10.1016/B978-0-444-53802-4.00037-3

Birch F (1952) Elasticity and constitution of the Earth's interior. Journal of Geophysical Research 57: 227-286, doi: 10.1029/JZ057i002p00227

Connolly JAD (2005) Computation of phase equilibria by linear programming: a tool for geodynamic modeling and its application to subduction zone decarbonation. Earth and Planetary Science Letters 236: 524-541, doi: 10.1016/j.epsl.2005.04.033

Cordier P and 5 coauthors (2014) Disclinations provide the missing mechanism for deforming olivine-rich rocks in the mantle. Nature 507: 51-56, doi: 10.1038/nature13043

Cordier P, Jackson JM (2026) More than math: how tensors help describe mineral properties. Elements 22: 74-76

Dziewonski AM, Anderson DL (1981) Preliminary reference Earth model. Physics of the Earth and Planetary Interiors 25: 297-356, doi: 10.1016/0031-9201(81)90046-7

Frenkel D, Smit B (1996) Understanding Molecular Simulation: From Algorithms to Applications. Academic Press Inc., 450 pp

Frolov T, Mishin Y (2010) Effect of nonhydrostatic stresses on solid-fluid equilibrium. I. Bulk thermodynamics. Physical Review B 82: 174113, doi: 10.1103/PhysRevB.82.174113

Gouriet K, Roussel P, Carrez P, Cordier P (2022) Ultimate mechanical properties of enstatite. Physics and Chemistry of Minerals 49: 30, doi: 10.1007/s00269-022-01206-5

Gratier JP, Dysthe DK, Renard F (2013) The role of pressure solution creep in the ductility of the Earth's upper crust. Advances in Geophysics 54: 47-179, doi: 10.1016/B978-0-12-380940-7.00002-0

Hobbs BE, Ord A (2016) Does non-hydrostatic stress influence the equilibrium of metamorphic reactions? Earth-Science Reviews 163: 190-233, doi: 10.1016/j.earscirev.2016.08.013

Jackson I (2015) Properties of rocks and minerals: physical origins of anelasticity and attenuation in rock. In: Schubert G (ed) Treatise on Geophysics (Second Edition). Elsevier, Oxford, pp 539-571, doi: 10.1016/B978-0-444-53802-4.00045-2

Jackson JM, Dobrosavljevic VV, Kenji O (2026) The heat is on: thermal transport and melting. Elements 22: 89-95

Langenhorst F, Deutsch A (2012) Shock metamorphism of minerals. Elements 8: 31-36, doi: 10.2113/gselements.8.1.31

Lenze A, Stöckhert B, Wirth R (2005) Grain scale deformation in ultra-high-pressure metamorphic rocks—an indicator of rapid phase transformation. Earth and Planetary Science Letters 229: 217-230, doi: 10.1016/j.epsl.2004.10.012

Mavko G, Mukerji T, Dvorkin J (2020) The Rock Physics Handbook (Third Edition). Cambridge University Press, 740 pp

Mazzucchelli ML, Moulas E, Schmalholz SM, Kaus BJP, Speck T (2026) Instability of fluid-mineral equilibrium under non-hydrostatic stress investigated with molecular dynamics. Journal of Geophysical Research: Solid Earth 131: e2025JB033520, doi: 10.1029/2025JB033520

Moulas E and 5 coauthors (2019) Relation between mean stress, thermodynamic, and lithostatic pressure. Journal of Metamorphic Geology 37: 1-14, doi: 10.1111/jmg.12446

Otzen C, Liermann HP, Langenhorst F (2023) Evidence for a rosiaite-structured high-pressure silica phase and its relation to lamellar amorphization in quartz. Nature Communications 14: 606, doi: 10.1038/s41467-023-36320-7

Powell R, Evans KA, Green ECR, White RW (2018) On equilibrium in non-hydrostatic metamorphic systems. Journal of Metamorphic Geology 36: 419-438, doi: 10.1111/jmg.12298

Prencipe M (2019) Quantum mechanics in Earth sciences: a one-century-old story. Rendiconti Lincei. Scienze Fisiche e Naturali 30: 239-259, doi: 10.1007/s12210-018-0744-1

Samae V and 8 coauthors (2021) Stress-induced amorphization triggers deformation in the lithospheric mantle. Nature 591: 82-86, doi: 10.1038/s41586-021-03238-3

Solomatova NV, Scheller EL, Trumbo SK (2026) Illuminated worlds: how spectroscopy lights the way in Earth and planetary sciences. Elements 22: 82-88

Stixrude L (2015) Seismic properties of rocks and minerals, and the structure of Earth. In: Schubert G (ed) Treatise on Geophysics (Second Edition). Elsevier, Oxford, pp 417-439, doi: 10.1016/B978-0-444-53802-4.00041-5

Turcotte DL, Schubert G (2002) Geodynamics. Cambridge University Press, 456 pp

Weidner T and 6 coauthors (2024) From electron tomography of dislocations to field dislocation mechanics: application to olivine. Modelling and Simulation in Materials Science and Engineering 32: 015004, doi: 10.1088/1361-651X/ad0a42

Wheeler J (2020) A unifying basis for the interplay of stress and chemical processes in the Earth: support from diverse experiments. Contributions to Mineralogy and Petrology 175: 116, doi: 10.1007/s00410-020-01750-9

Williamson ED, Adams LH (1923) Density distribution in the Earth. Journal of the Washington Academy of Sciences 13: 413-428

Wu X and 6 coauthors (2017) Seismic anisotropy of the D″ layer induced by (001) deformation of post-perovskite. Nature Communications 8: 14669, doi: 10.1038/ncomms14669

Zhong X and 5 coauthors (2021) Lower crustal earthquake associated with highly pressurized frictional melts. Nature Geoscience 14: 519-525, doi: 10.1038/s41561-021-00760-x ■